PHYSICAL REVIEW B VOLUME 59, NUMBER 10 1 MARCH 1999-II

# Origin of room-temperature perpendicular magnetic anisotropy in Ni/Pt multilayers

Young-Seok Kim and Sung-Chul Shin
*Department of Physics and Center for Nanospinics of Spintronic Materials, Korea Advanced Institute of Science and Technology, Taejon 305-701, Korea*
(Received 12 October 1998)

Room-temperature perpendicular magnetic anisotropy (PMA) was observed in Ni/Pt multilayer films having 7–30 Å Ni and constant 3 Å Pt sublayer thickness, prepared by magnetron sputtering at an Ar sputtering pressure of 7 mTorr. To understand the origin of PMA, the magnetoelastic anisotropy was determined from delicate *in situ* stress and *ex situ* magnetostriction coefficient measurements. Tensile stress, inversely decreased with the Ni sublayer thickness, was observed in all samples prepared at this sputtering pressure while the magnetostriction coefficient was found to be negatively increased as the Ni sublayer thickness increased. From the measurements of stress and magnetostriction coefficient, we have found the magnetoelastic anisotropy of $2.88-4.72\times10^5$ erg/cm$^3$ in the samples, which was large enough to overcome negative contributions from the surface and shape anisotropies. Thus, it could be concluded that the magnetoelastic anisotropy plays a major role in yielding PMA in this system. [S0163-1829(99)50110-0]

Current research on ultrathin magnetic films is largely focused on searching for multilayered systems exhibiting room-temperature perpendicular magnetic anisotropy (PMA), where the easy direction of magnetization is perpendicular to the film plane. Applications of these systems to high-density magnetic and magneto-optical recording have been attracting particular attention. For this purpose, Co- or Fe-based multilayer films prepared by alternate deposition of transition metal (Co or Fe) and nonmagnetic element (Pd, Ag, Pt, Au, etc.) have been extensively investigated: Most systems have been reported to have a strong PMA when the thickness of transition metal Co or Fe was thinner than a few monolayers.[1–7] The Néel's surface anisotropy as a consequence of the reduced symmetry at an interface[8] and enhanced magnetocrystalline anisotropy due to altered electronic structure[9,10] in a multilayer are considered to be the major origins for the observed PMA in Co- or Fe-based multilayer films: Thus, a positive interface contribution overcoming a negative volume one results in PMA in those systems.

In contrast, most Ni-based multilayers have been reported to show in-plane anisotropy at room temperature[7] and a theoretical investigation by Gay and Richter has also predicted in-plane anisotropy for monolayer Ni.[11] But very recently Shin *et al.* have reported room-temperature PMA in Ni/Pt multilayers having 7–26 Å Ni and 2.3–4.6 Å Pt layer thicknesses.[12] In this paper, we clarify the origin of the observed PMA in Ni/Pt multilayers by the determination of the magnetoelastic anisotropy from delicate *in situ* stress and *ex situ* magnetostriction measurements.

Ni/Pt multilayers were prepared by sequential dc magnetron sputtering onto glass substrates of $4\,\mathrm{cm}(l)\times1.1\,\mathrm{cm}(w)\times130\,\mu\mathrm{m}(t)$ at an Ar sputtering pressure of 7 mTorr. The multilayers had different Ni sublayer thicknesses of 7–30 Å but had the same Pt sublayer thickness of 3 Å and number of repeats of 30. The samples will be designated by $(t_{Ni}\,\mathrm{Ni}/t_{Pt}\,\mathrm{Pt})_n$, where $t_{Ni}$ is the thickness of the nickel sublayer, $t_{Pt}$ is the thickness of the platinum sublayer, and $n$ is the number of multilayer repeats.

Stress of Ni/Pt multilayers was measured *in situ* during the deposition using a homemade optical displacement detector. Details of the system have been described elsewhere.[13] Briefly, the displacement sensing probe, detecting a deflection of a substrate, was located behind the free end of the substrate in the cantilever geometry, where the back side of the substrate was coated by 1000-Å-thick Al. A change in the gap distance between the probe and the substrate, caused by stress of a film, was measured utilizing linearly changing response in the intensity of the reflected light with the gap distance. The sensitivity of the displacement probe was 132 mV/$\mu$m and the minimum detectable displacement was 7.6 Å using a voltmeter of 100 $\mu$V resolution: The probe turned out to be sensitive enough to detect displacement caused by a monoatomic layer deposition. Stress of a multilayer was determined from the change of the gap distance $\Delta d$ using a well-known Stoney's formula as follows:[14]

$$\sigma=\frac{E_s t_s^2}{3l^2(1-\nu_s)}\frac{\Delta d}{\Delta h}, \tag{1}$$

where $E_s$, $\nu_s$, $t_s$, and $l$ are Young's modulus, Poisson's ratio, thickness, and length of a substrate, respectively, and $\Delta h$ is the change of the film thickness. So, using $E_s=1.51\times10^{12}\,\mathrm{dyne/cm^2}$, $\nu_s=0.3$, $t_s=130\,\mu\mathrm{m}$, and $l=4\,\mathrm{cm}$ for glass substrate and assuming a monoatomic layer deposition of $\Delta h=2$ Å, a minimum detectable stress using the probe was estimated to be $2.9\times10^7$ dyne/cm$^2$.

The magnetostriction coefficient of multilayers was measured using the same displacement detecting system. The sample in the cantilever geometry was saturated along the film plane by an applied magnetic field up to 10 kOe and the saturation magnetostriction coefficient was determined using the following equation:[15,16]

$$\lambda=\frac{E_s t_s^2}{3l^2(1-\nu_s)}\frac{(1+\nu_f)\Delta d}{E_f t_f}, \tag{2}$$

 

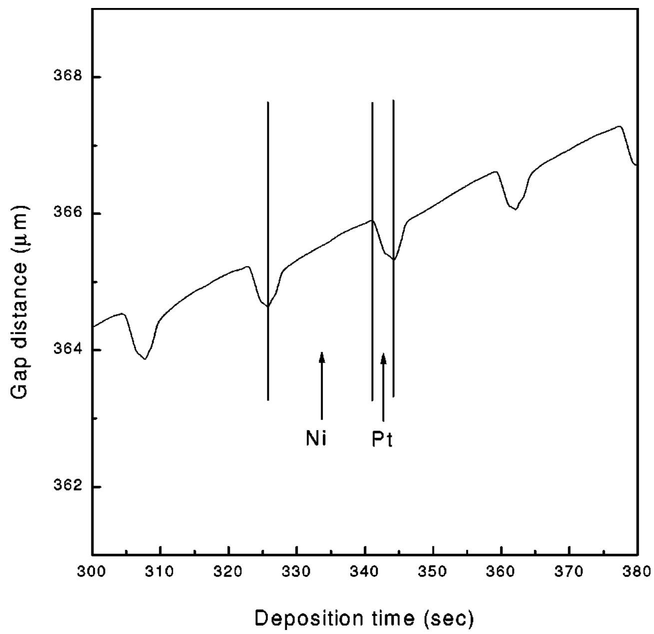


FIG. 1. A typical result of *in situ* stress measurement showing the gap distance variation with a function of the deposition time for a sample of (7-Å Ni/3-Å Pt)$_{30}$.

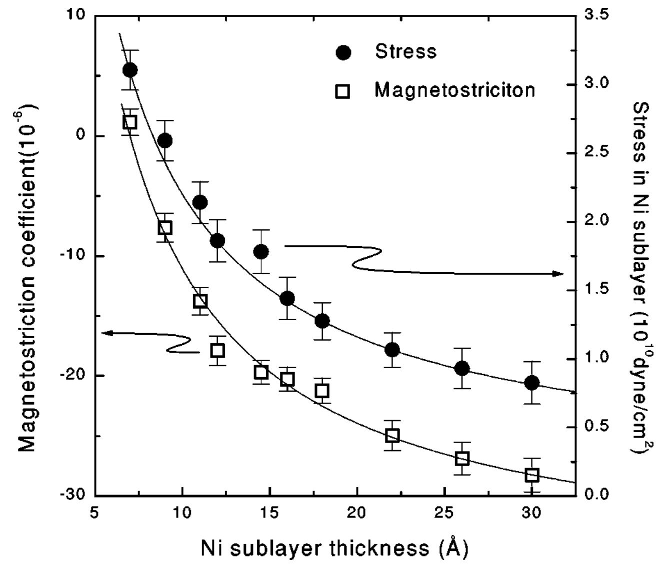


FIG. 2. A plot of the average stress and magnetostriction coefficient as a function of Ni sublayer thickness for a series of ($t_{Ni}$ Ni/3-Å Pt)$_{30}$ multilayers.

where $E_f$, $\nu_f$, and $t_f$ are Young's modulus, Poisson ratio, and thickness of a film, respectively. The resolution of the magnetostriction coefficient in this study was about $3.8 \times 10^{-7}$.

In Fig. 1, we demonstrate a typical plot of the gap distance vs the deposition time measured at every 50 ms for a sample of (7-Å Ni/3-Å Pt)$_{30}$. Here, the positive slope in the Ni sublayer and the negative slope in the Pt sublayer indicate the tensile and compressive stresses, respectively. This result is quite expected, since the *d* spacing of Ni in the (111) matching plane is 10.2% smaller than that of Pt. It is interesting to note from Fig. 1 that a large slope (i.e., a large tensile stress) in the Ni sublayer is developed at the beginning of the Ni-sublayer deposition on Pt and it relaxes to a moderate value before deposition of a half monolayer. We believe that this change of the slope is caused by a coherent-to-incoherent transition with Ni thickness. A larger stress is expected in the coherent matching system than in the incoherent one. The coherent matching in the (111) planes of Ni and Pt is expected only for Ni/Pt multilayers with very thin sublayer thickness due to a large lattice misfit. The critical Ni thickness of a coherent-to-incoherent transition is theoretically estimated to be 1.2 Å,[7] which is consistent with the experimental observation in Fig. 1.

Figure 2 shows a plot of stress and magnetostriction coefficient as a function of the Ni sublayer thickness. Here, the value of stress is obtained from averaging the stress existing in each Ni sublayer calculated using Eq. (1) and the error bar corresponds to the variation of the stress in each sublayer. Stress in the Ni sublayer was tensile in all samples and inversely proportional to the Ni sublayer thickness, which again revealed the incoherent growth of Ni sublayer on Pt. In general, there are three possible sources of stress in a multilayer film caused by a difference of thermal expansion coefficient between the substrate and the film, sputtering process, and lattice mismatch of two constituents at the interface. We refer to these stresses as thermal stress, process stress, and incoherency stress, respectively. The thermal stress in Ni/Pt multilayers was estimated to be $6.4 \times 10^8$ dyne/cm$^2$ and thus, its contribution to the total stress of the samples could be negligible compared with other stresses. The process stress measured for a single film of Ni was $6.5\times 10^9$ dyne/cm$^2$. Figure 2 shows that the average stress eventually approaches the value of the process stress of pure Ni film with increasing Ni sublayer thickness. Therefore, only the process stress seems to exist in Ni/Pt multilayers having thick Ni sublayers. This is quite expected since the incoherency stress is inversely proportional to the Ni sublayer thickness.

While with decreasing Ni sublayer thickness the magnetostriction coefficient was observed to decrease in magnitude and became nearly zero at 7-Å-thick Ni sublayer, with increasing Ni sublayer thickness it approached a bulk value of $2.8\times 10^{-5}$. It therefore could be conjectured that the surface magnetostriction coefficient[17] is positive and becomes dominant with decreasing Ni sublayer thickness in the Ni/Pt multilayer system.

Using the data in Fig. 2 the stress-induced magnetoelastic anisotropy $K_\lambda$ was determined utilizing the relation of $K_\lambda = -3/2\lambda\sigma$, and the magnetoelastic anisotropy of $2.88 \sim 4.72\times 10^5$ erg/cm$^3$ was obtained in our samples. In Fig. 3, we plot the magnetoelastic anisotropy vs the Ni sublayer thickness, together with the effective magnetic anisotropy measured using a torque magnetometer. It can be seen from the figure that the magnetoelastic anisotropy is larger than the effective magnetic anisotropy by a factor of about 3 in all samples showing PMA. One could notice that the peculiar dependence of the effective magnetic anisotropy on the Ni sublayer thickness originates from the magnetoelastic anisotropy depending on the Ni sublayer thickness.

The effective magnetic anisotropy $K_u^{\mathrm{eff}}$ in Ni/Pt multilayers could be modeled phenomenologically by $K_u^{\mathrm{eff}}=K_\lambda+K_d+K_c+2K_s/t_{Ni}$, where $K_d$ is the shape anisotropy, $K_c$ is the magnetocrystalline anisotropy, and $K_s$ is the surface anisot-

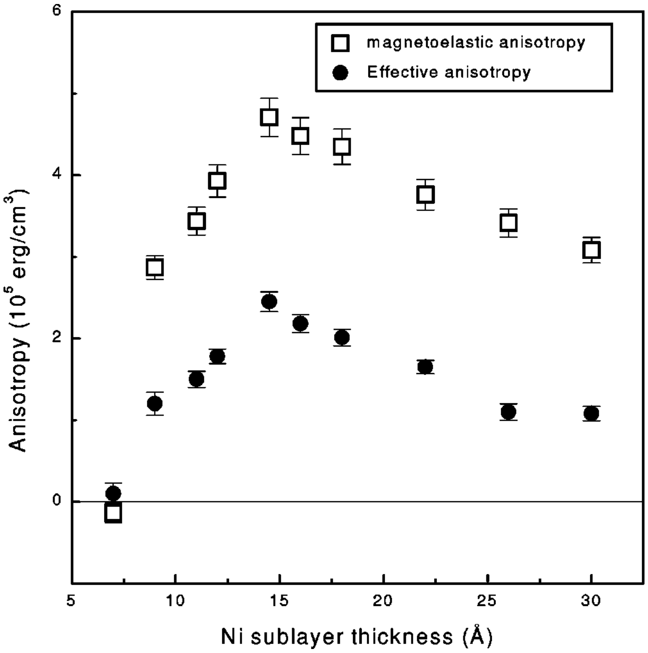


FIG. 3. The calculated magnetoelastic anisotropy vs Ni sublayer thickness, together with the effective magnetic anisotropy.

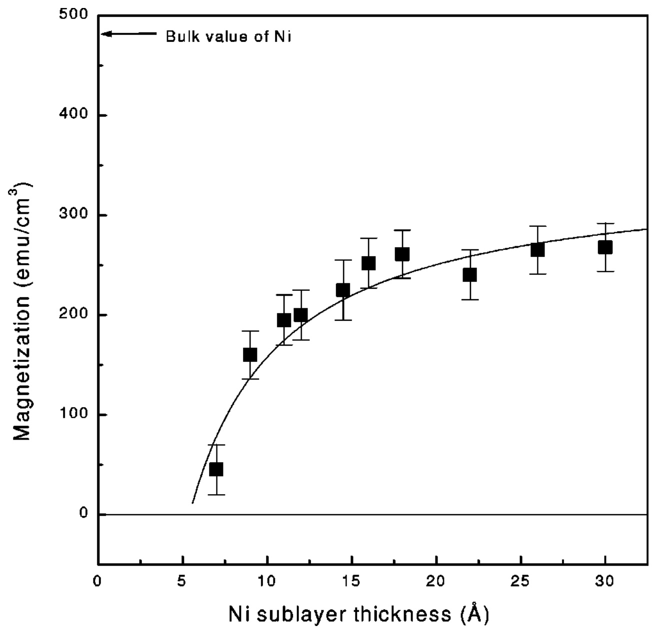


FIG. 4. Dependence of the saturation magnetization $M_s$ on $t_{Ni}$ in the ($t_{Ni}$ Ni/3-Å Pt)$_{30}$ multilayers. The sold line was obtained using the relation of $M = M_0(1-2\delta/t_{Ni})$.

ropy. Since $K_d$ is given by $-\alpha M_s^2$, where $\alpha$ is the demagnetization factor and $M_s$ is the saturation magnetization, both quantities should be known to estimate $K_d$. The $\alpha$ is $2\pi$ for a perfectly flat film, but it is structure sensitive and becomes smaller than $2\pi$ for an imperfect film having a rough surface.[18] We have determined the demagnetization factor in our samples by numerical calculation of the magnetic dipolar energy, considering real surface topology obtained from AFM measurement. It was found that $\alpha$ was reduced to 83% compared to that of a perfect film. Details of the calculation will be published elsewhere.[19] The saturation magnetization was measured using a vibrating sample magnetometer. The saturation magnetization at room temperature was found to inversely decrease with decreasing Ni sublayer thickness and it became zero when the Ni sublayer thickness was smaller than 6 Å. In Fig. 4 we plot the saturation magnetization $M_s$ as a function of the Ni sublayer thickness $t_{Ni}$ for the multilayers of ($t_{Ni}$Ni/3-Å Pt)$_{30}$. From these data, together with the theoretical calculation of $\alpha$, we have estimated $K_d$ of 0 to $-3.73\times10^5$ erg/cm$^3$ in our samples.

It is worthwhile to point out from Fig. 4 that the dependence of $M_s$ on $t_{Ni}$ strongly indicates the existence of interfacial effects in the Ni/Pt multilayers. We believe that the magnetic moment of the Ni sublayer adjacent to the Pt sublayer is suppressed due to an overlapping between the $d$ band of Ni and the conduction band of Pt.[20,21] Therefore, Ni sublayers near the interfaces are expected to be nonmagnetic or less magnetic. In this circumstance the magnetization of the Ni sublayer in a multilayer might be expressed by a simple relationship of $M = M_0(1-2\delta/t_{Ni})$, where $M$ is the Ni magnetization of a multilayer, $M_0$ is the magnetization of bulk Ni, and $\delta$ is the thickness of the nonmagnetic layer. Here, the factor 2 accounts for two interfaces for each Ni sublayer. Using this relationship we could well fit the dependence of the magnetization on the Ni sublayer thickness in Ni/Pt multilayers. The solid line in Fig. 4 was obtained from this equation with the values of $M_0 = 343\pm32$ emu/cm$^3$ and $\delta = 2.7 \pm 0.6$ Å. This thickness of the nonmagnetic Ni sublayer is consistent with the experimental observation that the magnetization is zero for the Ni sublayer thinner than 6 Å.

Since the value of $(K_u^{\mathrm{eff}} - K_d - K_\lambda)$ is equal to $(K_c + 2K_s/t_{Ni})$ in the phenomenological model, we plot $(K_u^{\mathrm{eff}} - K_d - K_\lambda)$ vs $1/t_{Ni}$ in Fig. 5 to examine the contributions of the magnetocrystalline and surface anisotropies. As seen in the figure this value increases with decreasing $1/t_{Ni}$ and it approaches the magnetocrystalline anisotropy of bulk Ni for the samples having $t_{Ni} \geqslant 18$ Å. So, it is believed that $K_c$ of $\sim 4.5\times10^4$ erg/cm$^3$ exists in our samples, but it is about ten

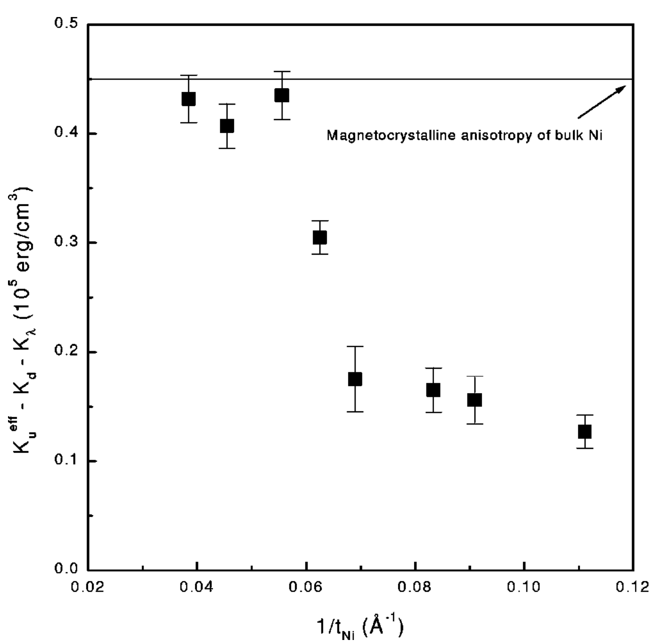


FIG. 5. A plot of $(K_u^{\mathrm{eff}} - K_d - K_\lambda)$ as a function of $1/t_{Ni}$.

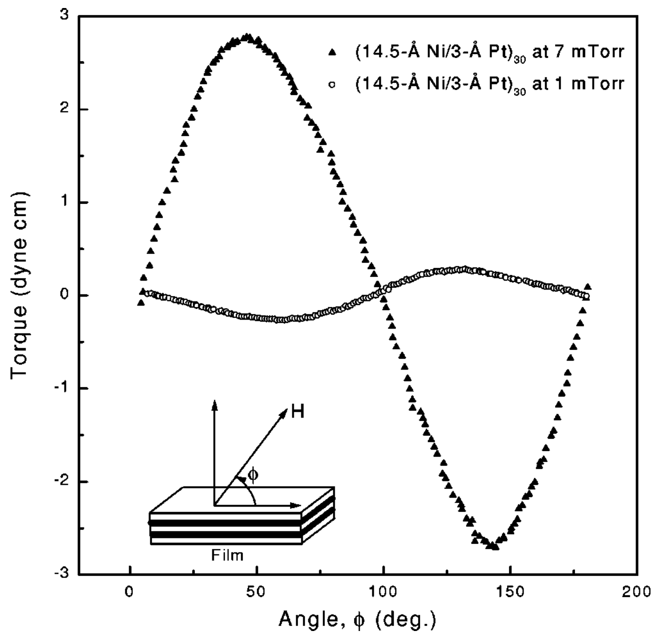


FIG. 6. Torque curves of two samples with the same composition of $(14.5\text{-Å Ni}/3\text{-Å Pt})_{30}$, but made under different Ar pressures of 1 and 7 mTorr.

times smaller than a typical value of $K_\lambda$ observed in the samples. The decreasing trend in the value of $(K_u^{\mathrm{eff}}-K_d-K_\lambda)$ with increasing $1/t_{Ni}$ implies a negative contribution of the surface anisotropy to the magnetic anisotropy of the samples. It therefore can be concluded that a positive magnetoelastic anisotropy overcoming negative contributions of the shape and surface anisotropies yields perpendicular magnetic anisotropy observed in our samples.

If our assertion that the stress-induced magnetoelastic anisotropy plays a major role in the magnetic anisotropy of Ni/Pt multilayers were true, one might naturally expect in-plane anisotropy for the samples having compressive stress in the Ni sublayers, assuming that the magnetostriction coefficient remains negative. To test this scenario we have engineered stress in the Ni sublayer by varying an Ar sputtering pressure during the sample preparation, and we obtained a compressive-stress sample prepared at an Ar sputtering pressure of 1 mTorr. In Fig. 6 we demonstrate two torque curves of $(14.5\text{-Å Ni}/3\text{-Å Pt})_{30}$ multilayers prepared at different Ar sputtering pressures of 1 and 7 mTorr. The sample made at an Ar sputtering pressure of 1 mTorr, which has compressive stress in the Ni sublayer, clearly shows in-plane anisotropy, whereas the sample made at an Ar sputtering pressure of 7 mTorr exhibits perpendicular magnetic anisotropy. This result provides further crucial evidence that the magnetoelastic anisotropy is mainly responsible for perpendicular magnetic anisotropy observed in our Ni/Pt multilayers.

In summary, we have investigated the origin of the room-temperature PMA in Ni/Pt multilayers fabricated at an Ar pressure of 7 mTorr. By careful determination of the magnetoelastic anisotropy from stress and magnetostriction measurements, we have found that PMA of this system originated from the magnetoelastic anisotropy induced by tensile stress in the samples. The tensile stress in Ni layer was due to the multilayer structure which reset the incoherent growth of Ni every bilayer period. The behavior of the effective magnetic anisotropy with varying Ni sublayer thickness was quantitatively explained by a phenomenological model considering the magnetoelastic, magnetocrystalline, shape, and surface anisotropies.

This work was supported by Creative Research Initiatives of the Korean Ministry of Science and Technology and the Center for Interface Science and Engineering of Materials.

[1] P. F. Carcia, A. D. Meinholdt, and A. Suna, Appl. Phys. Lett. **47**, 178 (1985).
[2] F. J. A. den Broeder, D. Kuiper, A. P. van de Mosselaer, and W. Hoving, Phys. Rev. Lett. **60**, 2769 (1988).
[3] D. G. Stinson and S.-C. Shin, J. Appl. Phys. **67**, 4459 (1990).
[4] B. Heinrich, J. F. Cochran, M. Kowakwski, J. Kisrschner, Z. Celinski, A. S. Arrott, and K. Myrtle, Phys. Rev. B **44**, 9348 (1991).
[5] M. Sakurai, Phys. Rev. B **50**, 3761 (1994).
[6] S. C. Shin, Appl. Surf. Sci. **65/66**, 110 (1993).
[7] M. T. Johnson, P. J. H. Bloemen, F. J. A. den Broeder, and J. J. deVries, Rep. Prog. Phys. **59**, 1409 (1996).
[8] L. Néel, J. Phys. Radium **15**, 225 (1954).
[9] L. Zhong, M. Kim, X. Wang, and A. J. Freeman, Phys. Rev. B **53**, 9770 (1996).
[10] X. Wang, R. Wu, D. Wang, and A. J. Freeman, Phys. Rev. B **54**, 61 (1996).
[11] J. G. Gay and Ray Richter, Phys. Rev. Lett. **56**, 2728 (1986).
[12] S.-C. Shin, G. Srinivas, Y.-S. Kim, and M.-G. Kim, Appl. Phys. Lett. **73**, 393 (1998).
[13] Y.-S. Kim and S.-C. Shin, Thin Solid Films **258**, 128 (1995).
[14] G. G. Stoney, Proc. R. Soc. London, Ser. A **A82**, 172 (1909).
[15] M. Weber, R. Koch, and K. H. Rieder, Phys. Rev. Lett. **73**, 1166 (1994).
[16] A. Hernando, A. Neuweiler, P. Farber, and H. Kronmüller, Phys. Rev. B **57**, 7458 (1998).
[17] G. Bochi, C. A. Ballentine, H. E. Inglefield, C. V. Thompson, and R. C. O'Handley, Phys. Rev. B **53**, R1729 (1996).
[18] T. Suzuki, H. Notarys, D. C. Dobertin, C.-J. Lin, D. Weller, D. C. Miller, and G. Gorman, IEEE Trans. Magn. **28**, 2756 (1992).
[19] Sug-Bong Choe and Sung-Chul Shin (unpublished).
[20] J. Tersoff and L. M. Falicov, Phys. Rev. B **26**, 6186 (1982).
[21] P. Chubing, D. Daosheng, and He Yongbing, J. Magn. Magn. Mater. **110**, 113 (1992).